

Examining the effectiveness of tropospheric correction methods on improving InSAR displacement measurements

Sahar Madahi, Seyed Rohallah Emadi

Abstract

The tropospheric effect is a significant error source in radar observations. To accurately calculate displacement fields, it is essential to apply advanced techniques to mitigate the tropospheric effect in the interferograms. This study examines land subsidence in Tehran province, Iran, using Sentinel-1A data from 2014 to 2021. Methods such as the Generic Atmospheric Correction Online Service (GACOS), ray tracing, and a new integration method were utilized to estimate the tropospheric effect. The integration method and ray tracing technique employed ERA5 reanalysis data from the European Centre for Medium-Range Weather Forecasts (ECMWF). In the final stage, the InSAR interferograms were refined using tropospheric corrections derived from these methods. Comparison of the subsidence data obtained from the three tropospheric correction techniques with Global Positioning System (GPS) observations showed that the results were closely aligned. However, the subsidence velocity derived from the new integration approach proved to be the most accurate.

Keywords: InSAR, Tropospheric Correction, Ray Tracing, Subsidence

23 1. Introduction

Natural and human activities such as tectonic plate movements, volcanic activity, earthquakes, and changes in groundwater levels can lead to vertical deformation of the Earth's surface, known as subsidence. Efforts have been made to forecast and monitor groundwater level depletion using machine learning (Haji-Aghajany et al., 2023) and to predict subsidence using similar methods (Tasan et al., 2023). Regular and optimal monitoring of subsidence can help prevent hazards in both residential and natural areas. In recent years, factors such as industrial activities and population growth have led to excessive groundwater extraction, resulting in aquifer depletion and subsequent land subsidence in various regions. These depletions are significant contributors to displacement and can cause subsidence of up to 17 cm in some areas (Gumilar et al., 2015). The primary cause of global subsidence is the change in groundwater levels, influenced by natural parameters and human activities, including precipitation, groundwater extraction, and soil absorption. Subsidence, the gradual or sudden downward movement of the Earth's surface, can pose serious risks to the stability of aquifers and human-made structures, making the study and monitoring of subsidence crucial worldwide.

Iran has faced significant spatiotemporal limitations in groundwater resources in recent years, primarily due to extensive extraction for industrial activities and urban development (Motagh et al., 2008). This paper focuses on an area south of Tehran in Tehran province, Iran. Land subsidence in this region can be studied using hydrogeological methods and geodetic tools such as GPS and InSAR (Abidin, 2008).

InSAR is a precise and powerful technique with high spatial resolution, capable of measuring Earth's surface displacement with millimeter accuracy (Ferretti et al., 2001). However, the

tropospheric effect is a major limiting factor in InSAR outputs (Zebker et al., 1997; Jolivet et al., 2014), necessitating its correction or reduction. Various tools are available for calculating the tropospheric effect, including meteorological data and radiosondes.

Numerous previous studies have focused on mitigating tropospheric effects using various approaches. One common method involves the interferometric combination of a series of radar images, assuming that the atmospheric effect is random over time while the displacement signal correlates with time (Ferretti et al., 2001; Tang et al., 2016). This approach employs temporal filtering of large radar image time series to eliminate atmospheric influences. Another approach relies on connected stacks of interferograms to characterize phase delay patterns (Foster et al., 2006; Lauknes, 2011). Additional methods analyze the relationship between elevation and tropospheric delay (Remy et al., 2003; Elliott et al., 2008) or utilize external meteorological data (Fournier et al., 2011; Dee et al., 2011; Jolivet et al., 2014). Recently, spectral diversity has been applied to reduce tropospheric effects (Jung and Lee, 2015; Fattahi et al., 2017; Mastro et al., 2020). Moreover, some researchers have employed three-dimensional (3D) and various two-dimensional (2D) ray tracing approaches (Haji-Aghajany et al., 2018; Haji-Aghajany et al., 2019; Haji-Aghajany and Amerian, 2020a), as well as outputs from numerical weather models (Haji-Aghajany and Amerian, 2020b). Troposphere tomography, a powerful technique for reconstructing water vapor, has also shown promise and has been applied in fields such as precipitation downscaling (Izanlou et al., 2024; Haji-Aghajany, 2021; Haji-Aghajany et al., 2022). In a recent study aimed at enhancing the accuracy of InSAR tropospheric corrections, Maddahi et al. (2024) utilized tomography to reduce tropospheric effects in InSAR measurements (Maddahi et al., 2024). This study reviews the impact of the tropospheric layer on InSAR measurements, using GACOS products, a ray tracing algorithm, and

a new integration method to calculate tropospheric delay. These computed delays are then applied to the radar interferograms. Finally, land subsidence estimates derived from the three tropospheric correction methods are compared with GPS measurements to assess their accuracy.

2. InSAR processing

The InSAR technique relies on phase extraction from radar images. By calculating the phase difference recorded in corresponding pixels of two radar images taken from the same area at different times, an interferogram is generated, which serves as the primary measurement in InSAR. The resulting interferogram contains a mixture of signals: deformation, topographical effects, orbital errors, tropospheric effects, and noise due to diffusion variations. The phase differences observed in the interferogram represent both the deformation signal and contributions from topographical changes, orbital errors, atmospheric effects, and diffusion changes (Hanssen, 2001):

$$\Delta\varphi = \Delta\varphi_{def} + \Delta\varphi_{atm} + \Delta\varphi_{topo} + \Delta\varphi_{orbit} + \Delta\varphi_{noise} \quad (1)$$

Where $\Delta\varphi_{def}$, $\Delta\varphi_{atm}$, $\Delta\varphi_{topo}$, $\Delta\varphi_{orbit}$ and $\Delta\varphi_{noise}$ are phase differences caused by deformation, tropospheric delay, topography, orbital error, and thermal noise, respectively. Since the goal of InSAR analysis is to compute deformation, other contributions to the InSAR phase must be removed. In this paper, the Shuttle Radar Topography Mission (SRTM) Digital Elevation Model (DEM) with a 10-meter resolution is used to mitigate the topographical effect, and orbital files are used to correct orbital errors. Intrusive parameters in InSAR measurements can significantly affect the calculated displacement fields caused by phenomena such as subsidence (Khalili et

al., 2023) or earthquakes (Haji-Aghajany et al., 2020). This study aims to explore methods for reducing these effects.

In the traditional InSAR method, only two radar images are used to calculate the deformation that occurred between the acquisition times of these images. To address the limitations of this approach, Persistent Scatterer Interferometry (PSI) and Small Baseline Subset (SBAS) algorithms have been developed to compute deformation time series using multi-temporal radar images (Berardino et al., 2002). These algorithms rely on a large number of images and persistent scatterers (PS) in the study area. The PSI method allows for the calculation of linear displacement velocity and the reconstruction of nonlinear time series for each PS. The SBAS algorithm, on the other hand, uses PSs that maintain coherence above a selected threshold across all interferograms (Samsonov, 2010). Both algorithms offer high accuracy in calculating deformation over time, represented as time series. Recently, InSAR processing methods have evolved to combine the strengths of the PSI and SBAS algorithms (Hooper et al., 2008).**3.**

Tropospheric effect mitigation

Tropospheric delay in radar signals arises from variations in tropospheric parameters such as pressure, temperature, and water vapor. As a radar signal traverses the troposphere, its velocity decreases, causing variable delays that affect observations (Jolivet et al., 2014). These variations can induce localized phase gradients in InSAR measurements, primarily due to changes in tropospheric parameters. Generally, temporal variations in pressure and temperature are not significant enough to create localized phase gradients in InSAR data (Hanssen, 1998). The primary factor influencing InSAR data is temporal changes in water vapor, which is typically present in the lower troposphere (Hanssen, 1998; Hanssen, 2001). Therefore, it is essential to compute these phase gradients caused by tropospheric variations.

3.1. Tropospheric correction using new integration technique

The tropospheric path delay in the zenith direction, known as the zenith tropospheric delay, is computed using numerical integration, which can be expressed as follows:

$$ZTD = 10^{-6} \left\{ \frac{k_1 R_d}{g_m} P(z_0) + \int_{z_0}^z \left(k_2 \frac{R_d}{R_v} k_1 \frac{e}{T} + k_3 \frac{e}{T^2} \right) dz \right\} \quad (2)$$

$k_1 = 0.776 KPa^{-1}$, $k_2 = 0.716 KPa^{-1}$, $k_3 = 3.75 \times 10^3 K^2 Pa^{-1}$

where z_0 is the height, z is the highest height of the troposphere, R_v (461.495 Jkg⁻¹K⁻¹) and R_d (287.05 Jkg⁻¹K⁻¹) are the specific gas constants for water vapor and dry air, respectively, $P(z_0)$ is the surface pressure, e is the water vapor pressure, T is the temperature in K, and g_m is the averaged gravitational acceleration. To mitigate the tropospheric effect from the radar signal, the zenith tropospheric delay must be converted to the line-of-sight direction (Cao et al., 2021). However, previous research has shown that this conversion, typically achieved using mapping functions, can introduce errors into the computation and final outputs. These errors may even result in misinterpreting the deformation signal in InSAR analysis. Therefore, this paper introduces a new, simplified integration method along the line-of-sight direction to circumvent errors associated with mapping functions in the results. Similar to the classic integration method along the zenith direction, this approach requires meteorological data in 3D space. The meteorological data along the line of sight are estimated using interpolation techniques. Figure 1 illustrates the comparison between the classic and new integration methods. In this study, spline interpolation is applied in the vertical direction, while kriging interpolation is used in the horizontal direction (Dubrule, 1984). For more detailed information about this method, please refer to Cao et al. (2021).

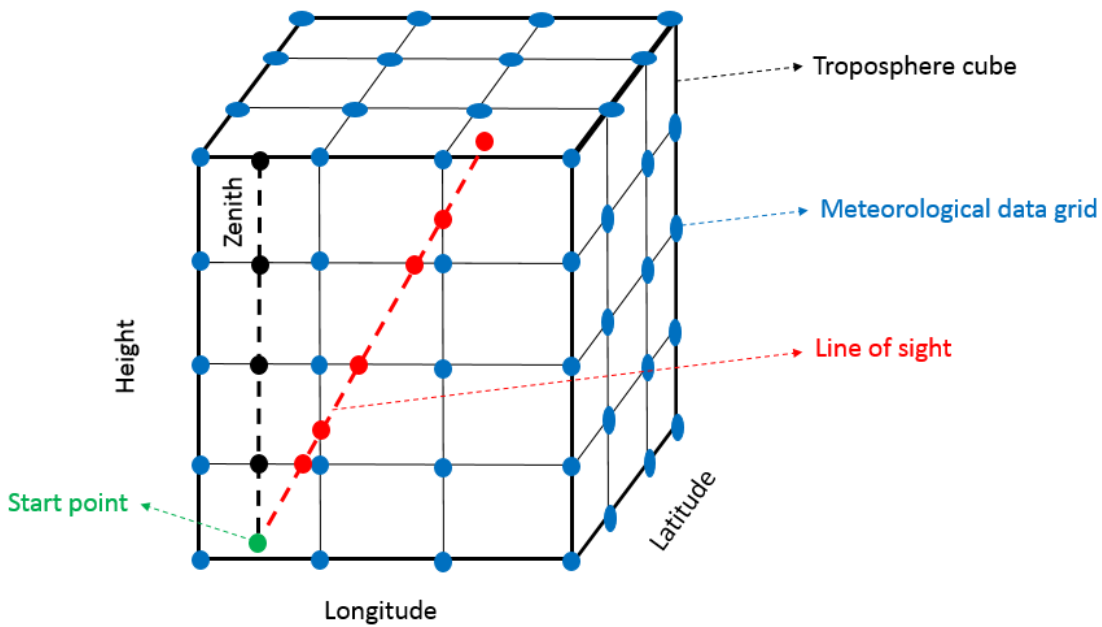


Figure 1. Comparison between classic integration and new mode (Khalili et al., 2023)

3.3. Tropospheric correction using GACOS products

The GACOS system, developed at Newcastle University in the United Kingdom, relies on meteorological data to address tropospheric delay in radar signals. It utilizes the 90 m resolution SRTM DEM (60° S - 60° N) and the Terra ASTER Global Digital Elevation Model (GDEM) in its processing. Additionally, GACOS integrates High-Resolution (HRES) datasets with spatial resolutions of up to 0.1° x 0.1° lat/long grid and 137 vertical pressure levels every 6 hours, derived from the European Centre for Medium-Range Weather Forecasts (ECMWF) (Xiao et al., 2021). Through the implementation of an iterative tropospheric decomposition model developed by Yu et al. (2018), GACOS separates stratified and turbulent components from tropospheric delays, producing high spatial resolution Zenith Total Delay (ZTD) maps. Yu et al. (2018) evaluated GACOS performance using various sites worldwide. Beyond theoretical and technological validations, GACOS offers a significant innovation in its operational mode: it provides a free online service, reducing barriers to InSAR tropospheric correction. Users only

need to submit a request with the location of their study region and radar data, and GACOS tropospheric products will be generated for them. Unlike GPS techniques that rely on ground measurements or meteorological data with potential delays of weeks, GACOS offers global coverage and near real-time availability.

3.2. Tropospheric correction using ray tracing method

The ray tracing method stands as a potent technique for accurately reconstructing the path of wave propagation using tropospheric indices, commonly employed in estimating tropospheric effects. These approaches are typically categorized into two classes: 2D and 3D algorithms (Hofmeister, 2016). In the 2D approach, ray tracing occurs within a plane with a fixed azimuth, while in the 3D method, the signal's path can be reconstructed in 3D space. One notable 2D ray tracing method is the piecewise-linear (PWL) algorithm, known for its adequate accuracy and high processing speed. This algorithm employs the refractive index at various tropospheric levels to apply Snell's law of refraction and compute the tropospheric effect, utilizing recursive relations for tropospheric delay computation (Hofmeister, 2016). Another refinement of the 2D ray tracing technique is the refined piecewise-linear (RPWL) algorithm, which enhances the accuracy of the PWL method by incorporating intermediate compression levels. This approach aims to improve the precision of ray tracing processes. Further insights into these methodologies and their application can be found in previous studies (Hofmeister, 2016). For this study, the RPWL algorithm is employed to compute the tropospheric delay.

4. Study area and data set

Since the 1960s, Tehran has experienced land subsidence, a phenomenon exacerbated by the city's burgeoning population, which now exceeds 15 million inhabitants. Situated in northern Iran, the Tehran plain spans 2,250 km² and is bounded by the Alborz Mountains to the north

and the Arad and Fashapouye mountains to the south. Land subsidence, primarily attributed to excessive groundwater extraction, predominantly affects the southwestern portion of the basin. Precise leveling operations initially revealed subsidence in this region. Tehran, Iran's capital, lies within a semiarid zone particularly susceptible to rapid land subsidence. Over recent years, subsidence in the Tehran Plain has encroached upon densely populated urban areas, particularly impacting the southern and southwestern sectors of the city (Esmaili and Motagh, 2016; Azadnejad et al., 2019). This area has endured significant adverse effects from land subsidence, primarily driven by excessive groundwater withdrawal. Numerous studies have investigated the extent of subsidence in Tehran (Ajourlou et al., 2019; Haghghi and Motagh, 2019; Azadnejad et al., 2019, 2020). The first attempt to estimate deformation in the Tehran Plain using the InSAR method was undertaken by Shemshaki et al. (2005). Figure 2 provides the geographical context of the study area.

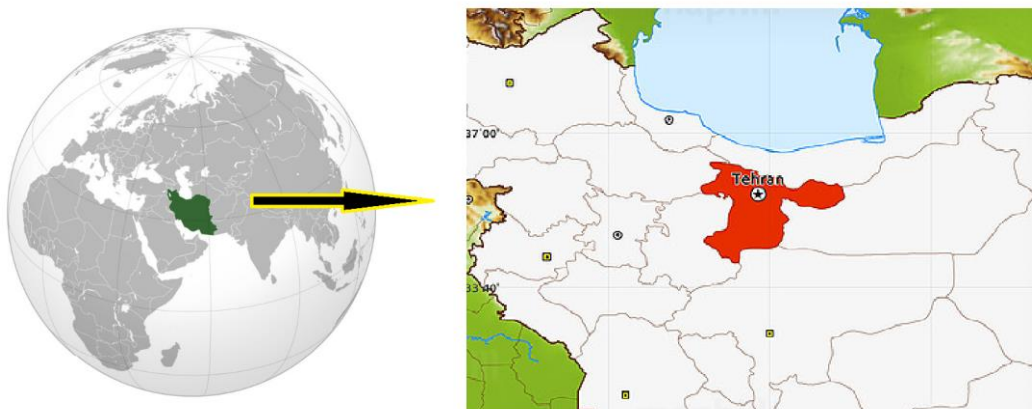


Figure 2. Location of the study area

To conduct the InSAR technique, a series of radar images captured by the Sentinel-1A satellite over two areas have been utilized. The specifications of the employed images are detailed in Table 1, while the spatiotemporal distribution is depicted in Figure 3. In this study, ERA5 reanalysis data from ECMWF has been employed for both ray tracing and new integration techniques. ERA5 provides reanalysis data

covering the period from 1950 to the present, furnishing meteorological data on 137 pressure levels from the surface up to 1 Pa (approximately 80 km). The spatial resolution of ERA5 data is approximately 31 km (Hersbach and Dee, 2016). For each radar image, the closest ERA5 data in time is selected. Temperature, pressure, and water vapor values at each pressure level are then interpolated. Kriging and spline interpolation methods are applied along the horizontal and vertical directions, respectively. Additionally, GPS observations are utilized to assess the derived displacement rates.

Table.1. Information of the used radar images

Beam Mode	IW
Path	28
Frame	112
Flight Direction	Ascending
Polarization	VV+VH
Absolute Orbit	44900
Date	16 Jan 2016 – 1 Jan 2021

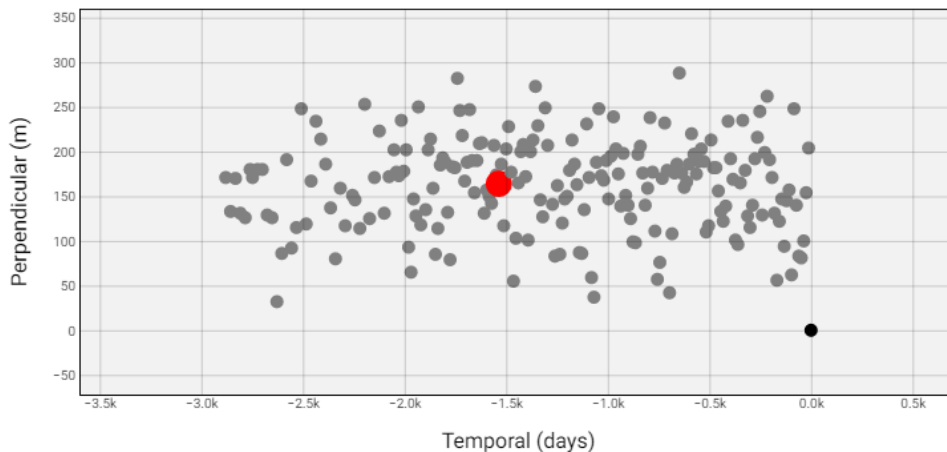


Figure 3. Spatiotemporal distribution of images

5. Processes

A series of Sentinel-1A radar images have been employed in the InSAR process utilizing the SBAS method. To estimate the displacement velocity field, intrusive effects must be mitigated or minimized from the calculated interferograms. Following the removal of topographical and orbital effects using DEM and orbital data, the remaining interferograms contain only tropospheric effects and deformation phase.

In this study, the tropospheric effect has been computed using the aforementioned methods, including the new integration algorithm, GACOS products, and ray tracing. Below, samples of computed tropospheric delay from these approaches can be observed in Figure 4.

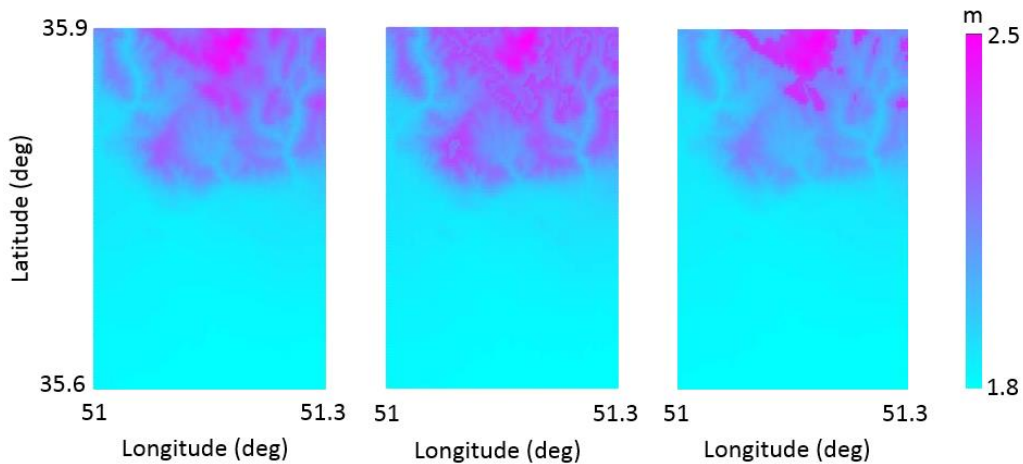


Figure 4. Samples of obtained tropospheric delay from new integration algorithm, GACOS products and ray tracing technique (left to right).

After applying the computed tropospheric delays to the obtained interferograms, the displacement rate of the study area has been determined (Figure 5). To facilitate comparison of the results, two separate profiles have been selected from the derived displacement velocity fields. Figure 6 illustrates that when employing the ray tracing method, numerous uplift and subsidence signals are observed across the study area. However, the utilization of GACOS products and the new integration technique has notably reduced the number of artificial signals. The presence of high displacement rates and a considerable number of signals in the displacement rate map obtained via the spatiotemporal filter method may be attributed to the lingering tropospheric effects in the obtained interferograms. Conversely, the use of the new integration technique and GACOS products could potentially mitigate both subsidence and uplift signals.

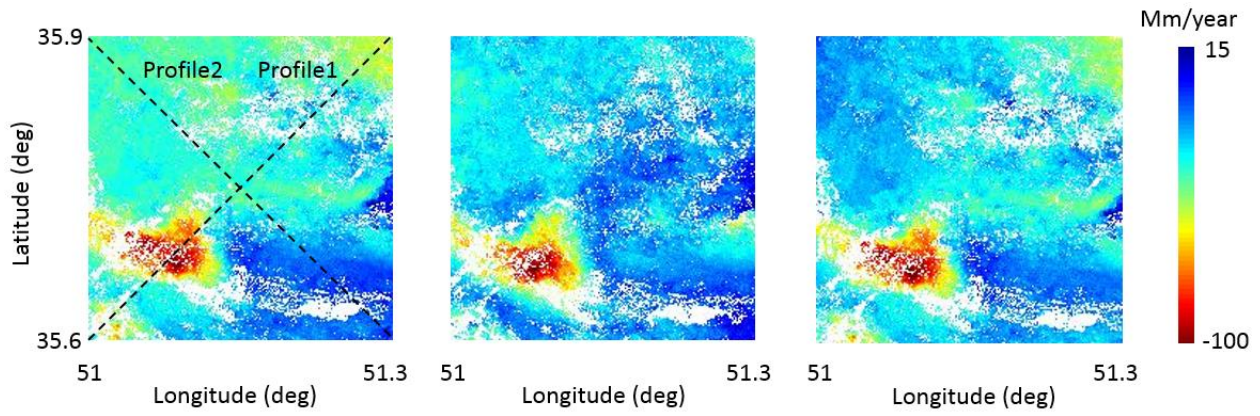


Figure 5. Obtained displacement velocity fields

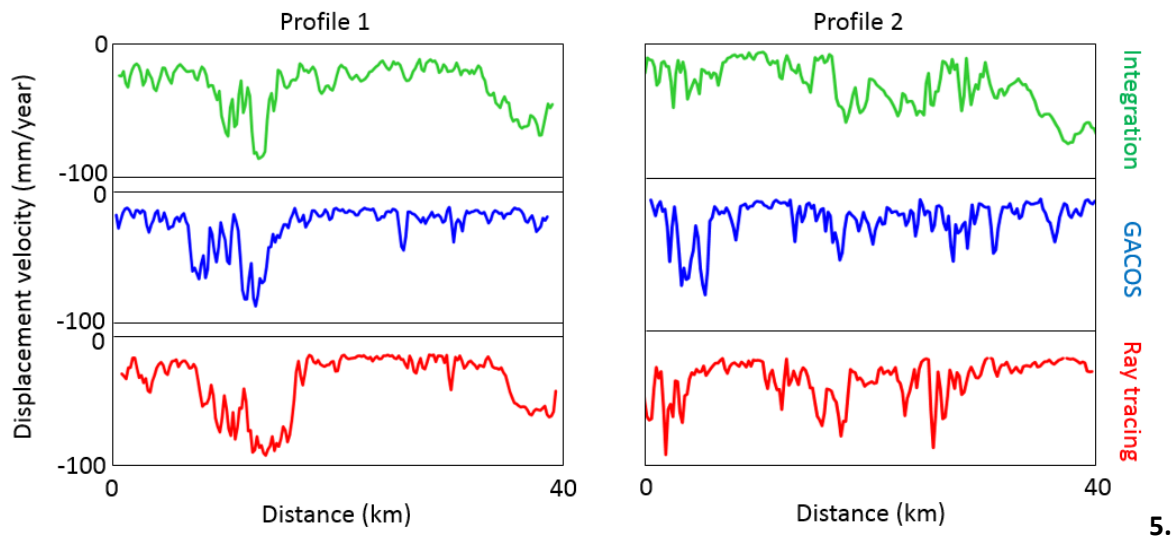


Figure 6. Considered profiles on the obtained displacement velocity maps

6. Validation with GPS observation

To assess the efficiency of the results, it is essential to compare the computed displacement velocities with the displacement rates derived from accurate measurements, such as GPS data. The validation using GPS data provides more accurate and reliable results due to the time interval overlap between the GPS data and radar images. To better evaluate the obtained results, the InSAR time series have been compared with the GPS time series. This comparison, conducted at the position of GPS stations, is depicted in Figure 7.

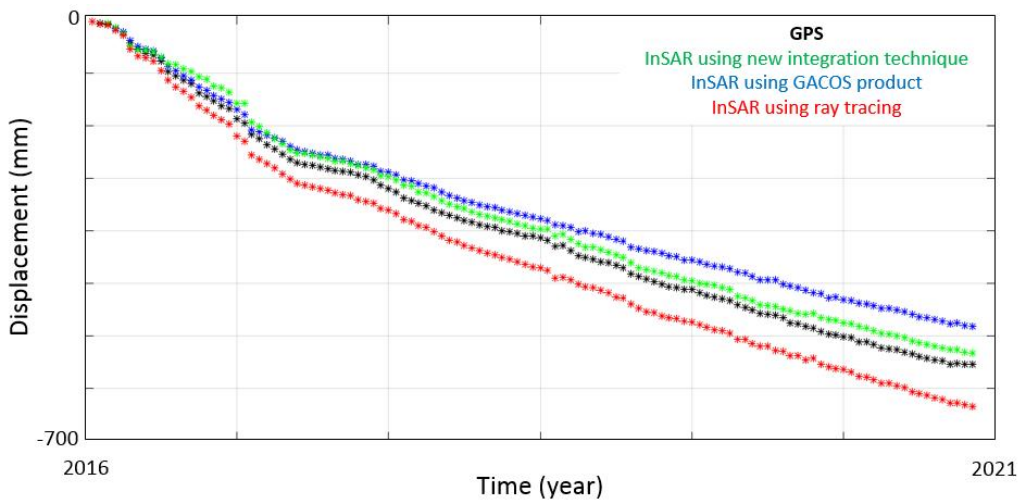


Figure 7. Samples of InSAR time-series and water level decline of four piezometric wells from up to down, respectively.

In order to comprehensively evaluate the mentioned methods, various statistical parameters have been computed. These statistical parameters, calculated to compare the obtained results with GPS observations, are presented in Table 2.

Table.2. Statistical parameters of different methods

Method	Mean absolute difference (mm)	Root mean square error (mm)
New integration	10.60	12.71
GACOS	21.22	16.89
Ray tracing	18.96	20.14

Based on the obtained results, it can be concluded that the new integration method demonstrates superior effectiveness in tropospheric calculations, leading to a more accurate displacement field compared to the other two approaches. Considering the expected accuracy of InSAR, which typically falls within millimeters, the differences observed in the results are statistically significant. However, it's important to note that implementing the new integration method and the ray tracing technique necessitates precise calculations and programming

efforts. In contrast, the use of GACOS products is notably simpler and faster, requiring minimal user calculations.

7. Conclusions

Tropospheric delay represents a significant constraint in radar measurements, capable of introducing errors of over one hundred millimeters to InSAR outputs. In this study, three methods—GACOS products, ray tracing technique, and the new integration approach—were compared to estimate tropospheric delay and enhance InSAR displacement accuracy. To investigate the impact of these approaches on InSAR displacement, a region was selected in the central part of Iran, within Tehran province. Following the computation of tropospheric correction using the aforementioned methods and subsequent correction of obtained interferograms, time series and displacement velocities were calculated. Ultimately, comparison of the outputs with GPS data revealed that the new integration technique yielded a more accurate displacement field compared to the other two approaches.

References

- Abidin, H. Z., Andreas, H., Gamal, M., Wirakusumah, A. D., Darmawan, D., Deguchi, T., & Maruyama, Y. (2008). Land subsidence characteristics of the Bandung Basin, Indonesia, as estimated from GPS and InSAR. *Journal of Applied Geodesy*, 2(3), 167-177.
- Ajourlou, P., Esfahany, S. S., & Safari, A. (2019). A new strategy for phase unwrapping in InSAR time series over areas with high deformation rate: case study on the Southern Tehran subsidence. *International Archives of the Photogrammetry, Remote Sensing & Spatial Information Sciences*, 42, 35–40.
- Azadnejad, S., Maghsoudi, Y., & Perissin, D. (2019). Investigating the effect of the physical scattering mechanism of the dual-polarization Sentinel-1 data on the temporal coherence optimization results. *International Journal of Remote Sensing*, 1, 15–7047. DOI: 10.1080/01431161.2019.1597309
- Azadnejad, S., Maghsoudi, Y., & Perissin, D. (2020). Evaluation of polarimetric capabilities of dual polarized Sentinel-1 and TerraSAR-X data to improve the PSInSAR algorithm using amplitude dispersion index optimization. *International Journal of Applied Earth Observation and Geoinformation*, 84, 101950. DOI: 10.1016/j.jag.2019.101950
- Berardino, P., Fornaro, G., Lanari, R., & Sansosti, E. (2002). A new algorithm for surface deformation monitoring based on small baseline differential SAR interferograms. *IEEE Transactions on Geoscience and Remote Sensing*, 40, 2375-2383.
- Cao, Y., Jónsson, S., & Li, Z. (2021). Advanced InSAR tropospheric corrections from global atmospheric models that incorporate spatial stochastic properties of the troposphere. *Journal of Geophysical Research: Solid Earth*, 126, e2020JB020952. DOI: 10.1029/2020JB020952
- Dee, D. P., and 35 co-authors. (2011). The ERA-Interim reanalysis: Configuration and performance of the data assimilation system. *Quarterly Journal of the Royal Meteorological Society*, 137(656), 553–597. DOI: 10.1002/qj.828
- Dubrulle, O. (1984). Comparing splines and kriging. *Computers & Geosciences*, 10, 327–338.

- Elliott, J., Biggs, J., Parsons, B., & Wright, T. J. (2008). InSAR slip rate determination on the AltynTagh Fault, northern Tibet, in the presence of topographically correlated atmospheric delays. *Geophysical Research Letters*, 35, L12309.
- Esmaeili, M., & Motagh, M. (2016). Improved Persistent Scatterer analysis using Amplitude Dispersion Index optimization of dual polarimetry data. *ISPRS Journal of Photogrammetry and Remote Sensing*, 117, 108–114. DOI: 10.1016/j.isprsjprs.2016.03.018
- Fattahi, H., Simons, M., & Agram, P. (2017). InSAR Time-Series Estimation of the Ionospheric Phase Delay: An Extension of the Split Range-Spectrum Technique. *IEEE Transactions on Geoscience and Remote Sensing*, 55, 5984–5996. DOI: 10.1109/TGRS.2011.2139217
- Ferretti, A., Prati, C., & Rocca, F. (2001). Permanent scatters in SAR interferometry. *IEEE Transactions on Geoscience and Remote Sensing*, 39(1), 8–20.
- Foster, J., Brooks, B., Cherubini, T., Shacat, C., Businger, S., & Werner, C. L. (2006). Mitigating atmospheric noise for InSAR using a high resolution weather model. *Geophysical Research Letters*, 33, L16304. DOI: 10.1029/2006GL026781
- Fournier, T., Pritchard, M. E., & Finnegan, N. (2011). Accounting for atmospheric delays in InSAR data in a search for long-wavelength deformation in South America. *IEEE Transactions on Geoscience and Remote Sensing*, 49(10), 3856–3867. DOI: 10.1109/TGRS.2011.2139217
- Gumilar, I., Abidin, H. Z., Hutasoit, L. M., Hakim, D. M., Sidiq, T. P., & Andreas, H. (2015). Land subsidence in Bandung Basin and its possible caused factors. *Procedia Earth and Planetary Science*, 12, 47-62.
- Haghighi, M. H., & Motagh, M. (2019). Ground surface response to continuous compaction of aquifer system in Tehran, Iran: results from a long-term multi-sensor InSAR analysis. *Remote Sensing of Environment*, 221, 534–550. DOI: 10.1016/j.rse.2018.11.003.
- Haji-Aghajany, S., & Amerian, Y. (2018). An investigation of three-dimensional ray tracing method efficiency in precise point positioning by tropospheric delay correction. *Journal of Earth and Space Physics*, 44, 39–52. DOI: 10.22059/JESPHYS.2018.236885.1006913
- Haji-Aghajany, S., Voosoghi, B., & Amerian, Y. (2019). Estimating the slip rate on the north Tabriz fault (Iran) from InSAR measurements with tropospheric correction using 3-D ray tracing technique. *Advances in Space Research*, 64(11), 2199–2208. DOI: 10.1016/j.asr.2019.08.021
- Haji-Aghajany, S., & Amerian, Y. (2020a). Atmospheric phase screen estimation for land subsidence evaluation by InSAR time series analysis in Kurdistan, Iran. *Journal of Atmospheric and Solar-Terrestrial Physics*, 209, 105314. DOI: 10.1016/j.jastp.2020.105314
- Haji-Aghajany, S., & Amerian, Y. (2020b). Assessment of InSAR tropospheric signal correction methods. *Journal of Applied Remote Sensing*, 14(4), 044503. DOI: 10.1117/1.JRS.14.044503
- Haji-Aghajany, S., Pirooznia, M., Raoofian Naeeni, M., & Amerian, Y. (2020). Combination of Artificial Neural network and Genetic Algorithm to inverse source parameters of Sefid-Sang earthquake using InSAR technique and Analytical model conjunction. *Journal of Earth and Space Physics*, 45(4), 121–131. DOI: 10.22059/JESPHYS.2019.269596.1007065
- Haji-Aghajany, S. (2021). Function-based troposphere water vapor tomography using GNSS observations. PhD Thesis, Faculty of Geodesy and Geomatics Engineering, Toosi University of Technology.
- Haji-Aghajany, S., Amerian, Y., & Amiri-Simkoei, A. (2022). Function-based troposphere tomography technique for optimal downscaling of precipitation. *Remote Sensing*, 14(11), 2548. DOI: 10.3390/rs14112548
- Haji-Aghajany, S., Amerian, Y., & Amiri-Simkoei, A. (2023). Impact of Climate change parameters on groundwater level: implications for two subsidence regions in Iran using geodetic observations and artificial Neural networks (ANN). *Remote Sensing*, 15, 1555. DOI: 10.3390/rs15061555

- Hanssen, R. (1998). Atmospheric heterogeneities in ERS tandem SAR interferometry. DEOS Report No.98.1, Delft University press: Delft, the Netherlands.
- Hanssen, R. (Ed.). (2001). Radar Interferometry, Data Interpretation and Error Analysis. Kluwer Academic Publishers, p. 308.
- Hersbach, H., & Dee, D. (2016). ERA5 Reanalysis is in Production. ECMWF Newsletter, 147. ECMWF: Reading, UK.
- Hofmeister, A. (2016). Determination of path delays in the atmosphere for geodetic VLBI by means of ray tracing. Vienna University of Technology, ISSN: 1811-8380.
- Hooper, A. (2008). A multi-temporal InSAR method incorporating both persistent scatterer and small baseline approaches. Geophysical Research Letters, 35, L16302.
- Izanlou, A. S., Haji-Aghajany, B. S., & Amerian, C. Y. (2024). Enhanced troposphere tomography: integration of GNSS and remote sensing data with optimal vertical constraints. IEEE Journal of Selected Topics in Applied Earth Observations and Remote Sensing.
- Jolivet, R., Agram, P. S., Lin, N. Y., Simons, M., Doin, M. P., Peltzer, G., & Li, Z. (2014). Improving InSAR geodesy using global atmospheric models. Journal of Geophysical Research: Solid Earth, 119, 2324–2341. DOI: 10.1002/2013JB010588
- Jung, H.-S., & Lee, W.-J. (2015). An Improvement of Ionospheric Phase Correction by Multiple-Aperture Interferometry. IEEE Transactions on Geoscience and Remote Sensing, 53, 4952–4960. DOI: 10.1109/TGRS.2015.2405695
- Khalili, M. A., Voosoghi, B., Guerriero, L., Haji-Aghajany, S., Calcaterra, D., & Di Martire, D. (2023). Mapping of mean deformation rates based on APS-corrected InSAR data using unsupervised clustering algorithms. Remote Sensing, 15(2), 529. DOI: 10.3390/rs15020529.
- Lauknes, T. R. (2011). InSAR Tropospheric Stratification Delays: Correction Using a Small Baseline Approach. IEEE Geoscience and Remote Sensing Letters, 8, 1070-1074.
- Maddahi, S., Tasan, M., & Haji-Aghajany, S. (2023). Enhancing InSAR accuracy: Unveiling more accurate displacement fields through 3-D troposphere tomography. Journal of Atmospheric and Solar-Terrestrial Physics, Volume 256. DOI: 10.1016/j.jastp.2024.106207
- Mastro, P., Serio, C., Masiello, G., & Pepe, A. (2020). The Multiple Aperture SAR Interferometry (MAI) Technique for the Detection of Large Ground Displacement Dynamics: An Overview. Remote Sensing, 12, 1189.
- Motagh, M., Walter, T. R., Sharifi, M. A., Fielding, E., Schenk, A., Anderssohn, J., & Zschau, J. (2008). Land subsidence in Iran caused by widespread water reservoir overexploitation. Geophysical Research Letters, VOL. 35, L16403.
- Remy, D., Bonvalot, S., Briole, P., & Murakami, M. (2003). Accurate measurement of tropospheric effects in volcanic areas from SAR interferometry data: application to Sakurajima volcano (Japan). Earth and Planetary Science Letters, 213, 299–310.
- Samsonov, S. (2010). Topographic Correction for ALOS PALSAR Interferometry. IEEE Transactions on Geoscience and Remote Sensing, 48, 3020-3027.
- Shemshaki, A. B., Blourchi, M. J., & Ansari, F. (2005). Earth subsidence review at Tehran plain-Shahriar (first report). http://gsi.ir/General/Lang_en/Page_27/GroupId_01-01/Typeld_All/Start_20/Action_ListView/Websiteld_13/3.html

- Tang, W., Liao, M. S., & Yuan, P. (2016). Atmospheric correction in time-series SAR interferometry for land surface deformation mapping - A case study of Taiyuan, China. *Advances in Space Research*, 58, 310-325. DOI: 10.1016/j.asr.2016.05.003
- Tasan, M., Ghorbaninasab, Z., Haji-Aghajany, S., & Ghiasvand, A. (2023). Leveraging GNSS tropospheric products for machine learning-based land subsidence prediction. *Earth Science Informatics*, 1–18.
- Zebker, H. A., Rosen, P. A., & Hensley, S. (1997). Atmospheric effects in interferometric synthetic aperture radar surface deformation and topographic maps. *Journal of Geophysical Research*, 102(2), 7547–7563.
- Xiao, R., Yu, C., Li, Z., & He, X. (2021). Statistical assessment metrics for InSAR atmospheric correction: applications to generic atmospheric correction online service for InSAR (GACOS) in eastern China. *International Journal of Applied Earth Observation and Geoinformation*, 96, Article 102289.
- Yu, C., Li, Z., Penna, N. T., & Crippa, P. (2018). Generic atmospheric correction model for interferometric synthetic aperture radar observations. *Journal of Geophysical Research: Solid Earth*, 123, 9202–9222. DOI: 10.1029/2017JB015305.